Taccone, Florent; Antoine, Germain

Numerical modeling of sediment transfers at the catchment scale with TELEMAC

Numerical modeling of sediment transfers at the catchment scale with TELEMAC

TACCONE Florent & ANTOINE Germain
Laboratoire National d'Hydraulique et Environnement
EDF R&D
Chatou, France
germain.antoine@edf.fr

Abstract— **The aim of this work focuses on the extension of the 2D code TELEMAC-SISYPHE from the river bed to the catchment scale. Several formulae have been implemented into the code in order to take into account erosion processes due to the rainfall. Furthermore, a continuous model, which estimates the friction coefficient directly as a function of the water level, has been implemented. These new developments are tested first on two theoretical test cases, representing two different scales: the first one represents processes at the plot scale, and the second one models two hillslopes adjacent to a straight river bed. Then the model is validated and calibrated on field data from a real catchment (Draix, in the Southern French Alps). These first results are very promising, and open new perspectives on the way of applying TELEMAC.**

INTRODUCTION

The transfers of sediments and associated contaminants play an important role in catchment management. An excessive sediment yield from hillslopes to river channels can contribute to reservoir siltation, degradation of aquatic habitats and to the export of nutrients or contaminants to downstream water bodies. However, the dynamics of sediment and contaminant redistribution is highly variable in space and time due to the complex non-linear processes involved. Because of this complexity and the huge spatial and temporal scales of the processes, few numerical models are today able to reproduce this transfer dynamic.

One of the main difficulties consists in representing continuously the flow and the erosion processes that are involved in every compartments of the watershed. Especially, a continuity between river flow and sheet flow has to be defined. Furthermore, it is necessary to represent the rain effect on the hillslope erosion, and to model properly the moderating effect of the water level on this specific erosion. From the hillslope to the river bed, many erosion processes may be involved, such as splash effect, rain fall induced transport or rain detachment with flow transport. In order to reproduce the effective sediment transport at the catchment scale, each one of these erosion processes has to be represented with the right order of magnitude.

In this work, a continuous model of the friction coefficient, calculated as a function of the water depth, has been implemented in TELEMAC-2D. Four rain detachment formulas have been also implemented in TELEMAC-SISYPHE, in order to take into account the effect of the rain as an additional source term in the advection-dispersion equation for suspended sediment transport. These new developments of the code, presented in the first part of this paper, have been evaluated on two test cases: one simple plot with a slope break for representing the local scale, and one straight river bed with two adjacent hillslopes for an intermediate scale. Then, data from a real watershed have been used to evaluate their relevance on a large scale by comparing the simulated results and the measurements. These results are presented in the second part, and discussed in the last part.

MATERIALS AND METHODS

All the simulations have been performed with the V7P0 version of TELEMAC-SISYPHE. The suspension sediment transport is calculated with the 2D advection-dispersion equation in the conservative form, and the source terms for erosion and deposition depend on the considered sediments. In this study, we focused on non-cohesive sediments. From a defined value of sediment diameter, the default parameters of the suspension simulation have been used. For non-cohesive sediments, the erosion and deposition terms are calculated as:

$$E - D = V_s(C - C_{eq})$$

with E the erosion rate ($m.s^{-1}$), D the deposition rate ($m.s^{-1}$), V_s the settling velocity calculated with the Soulsby formula, C the concentration of sediment in the flow and C_{eq} the equilibrium concentration evaluated with the Zyserman and Fredsoe formula (see the manual [1] for more informations).

Friction coefficient estimation

To represent the bottom friction, the model presented here has been defined in [2]. The inundation ratio Λ is a dimensionless number which is defined by the following formula:

$$\Lambda = \frac{h}{k}$$

with h the water depth and k the representative height of the soil roughness.

Using this parameter, the Darcy-Weisbach coefficient *f* is characterized by the equation:

$$f = \begin{cases} \left(\frac{1}{1.64 + 0.803\ln(\Lambda)}\right)^2 \; if\ \Lambda \geq 10 \\ \frac{10}{\Lambda} \; if\ 1 \leq \Lambda < 10 \\ \frac{192}{\pi R_*} min\left(\frac{\pi}{4}, \Lambda\right) \; else \end{cases}$$

with R_* the Reynolds number associated to a particle.

Finally, the Chezy coefficient C ($m^{1/2}.s^{-1}$) is given by:

$$C = \sqrt{\frac{8g}{f}}$$

With g the gravity acceleration in $m.s^{-2}$.

We can notice that for very small values of Λ, the friction is representative of a sheet flow around spherical structures.

Rain erosion

Four formulas have been chosen from existing erosion codes (PSEM_2D [3], WESP [4], EUROSEM [5] and FullSWOF_2D [6]) in order to reproduce the detachment due to rain drop impacts:

- $E1 = \alpha_r R\left(1 - \frac{h}{6.69R^{0.182}}\right)$
  with α_r the erodability coefficient ($kg.m^{-2}.mm^{-1}$), R the rain intensity ($m.s^{-1}$) and h the water depth (mm).
- $E2 = K_i R^2$
  with K_i the erodability coefficient ($kg.m^{-4}.s^{-1}$) and R the rain intensity ($m.s^{-1}$).
- $E3 = \frac{k}{\rho_s}(8.95 + 8.44\log(R))\ e^{-2h}$
  with k the erodability coefficient ($g.J^{-1}$), ρ_s the density of sediments ($kg.m^{-3}$), R the rain intensity ($m.s^{-1}$) and h the water depth (m).
- $E4 = \alpha\frac{h_0}{h}R$
  with α the erodability coefficient ($kg.m^{-3}$), h_0 the minimal value of the water depth to drag sediments (m), h the water depth (m) and R the rain intensity ($m.s^{-1}$).

An important point to notice is that the moderating effect of the water level h on the rain drop impacts is taken into account in E1, E3 and E4 by different ways.

These equations are implemented into SISYPHE as an additional source term for erosion in the advection-dispersion equation for suspended sediment transport.

Hairsine and Rose model

Another complete model for erosion and deposition is tested. In the Hairsine and Rose model, described in [7], the continuity equations for suspension and for bed evolution are the same as in SISYPHE, with different source terms for erosion and deposition. In this model, a deposited layer is introduced and is governed by the equation:

$$\frac{\partial M}{\partial t} = D - E_{fd} - E_{rd}$$

where M is the mass of the deposited layer ($kg.m^{-2}$), D the deposition rate ($kg.m^{-2}.s^{-1}$), E_{fd} and E_{rd} ($kg.m^{-2}.s^{-1}$) the detachment of the deposited layer due to respectively the flow and the rain.

In addition to the three source terms representing the evolution of the deposited layer, there are two erosion terms that influence the original soil E_r and E_f. These 5 source terms for both original soil and deposited layer are detailed bellow:

- $D = Ch\left(1 - e^{\frac{-V_s dt}{h}}\right)$
- $E_r = (1 - H)\alpha R\frac{h_0}{h}$
- $E_{rd} = H\alpha_d R\frac{h_0}{h}$
- $E_f = (1 - H)\frac{F(\omega - \omega_c)}{J}$
- $E_{fd} = HF(\omega - \omega_c)\frac{\rho_s}{(\rho_s - \rho)gh}$

where C is the mass concentration ($kg.m^{-3}$), h the water depth (m), V_s the settling velocity ($m.s^{-1}$), dt the time step (s), α and α_d are erodability coefficients respectively for original soil and deposited layer ($kg.m^{-3}$), R is the rain intensity ($m.s^{-1}$), ω-ω_c the available stream power ($m^2.s^{-1}$), F a fraction, g the gravity acceleration ($m.s^{-2}$), ρ the water density ($kg.m^{-3}$) and ρ_s the sediment density ($kg.m^{-3}$). The high number of parameters is the main characteristic of this model, therefore its calibration might be difficult.

Theoretical test cases

To test these developments, a very intensive rain (100 $mm.h^{-1}$) is simulated on two domains (Fig. 1) during one hour.

The first test case is a 4×1 m parcel, with a 10% slope upstream, a slope break in the middle and a 1% slope downstream. The size of the mesh is 1 cm and a water height of 3 mm is imposed at the downstream boundary. The chosen constant value of the Chezy coefficient is 28.

The second one is a river with two adjoining 20 m hillslopes with a 10% slope. A discharge of 1 $m^3.s^{-1}$ is imposed upstream, then flowing over 50 m following a 1% slope, to a reservoir with a 3 m weir downstream. The river is considered as a non-erodible zone. The Chezy coefficient for the constant bottom friction model is 40 and the chosen size of the mesh is 15 cm.

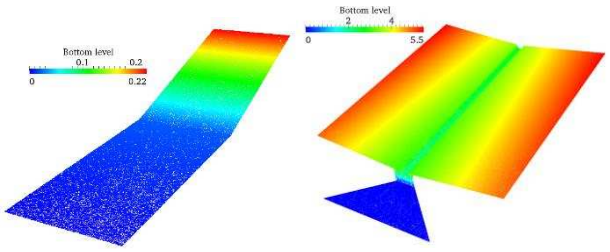

(a) : 4×1 m parcel (b) : River with adjacent parcels

Figure 1: Representation of the bottom level (m) for the two theoretical test cases

For both test cases, the size of the non-cohesive sediments in the model is 150 µm, this value is used as the representative height of the soil roughness. In every node of the mesh, a random number between -1 mm and 1 mm, following a uniform distribution, is added to the bottom elevation to create a disturbance in order to be more representative of a real soil.

Real case

Thanks to data provided by [8], it is possible to evaluate these new developments by comparing results from SISYPHE to measured discharges and suspended sediment concentrations from field campaigns on a real catchment.

The Laval watershed (Fig. 2) is a sub-catchment of the Bouinenc watershed, located on the Draix site in the Southern French Alps. Its total area is about 86.4 ha. The soil is mostly constituted of black marls and half of the surface is a bare soil. At the outlet of the catchment, the discharge and the associated sediment concentration are available for many rainfall events.

First the same constant one-hour rain is performed on the whole watershed in order to evaluate the model at this scale. Then two fast and intensive rainfall events are chosen in order to calibrate and validate the new developments. The hydraulic part of the model is calibrated using different size of the surface roughness, which is the k parameter in the inundation ratio used for the friction model. Indeed, the main river bed contains bigger irregularities, thus a specific value of k is defined in this zone.

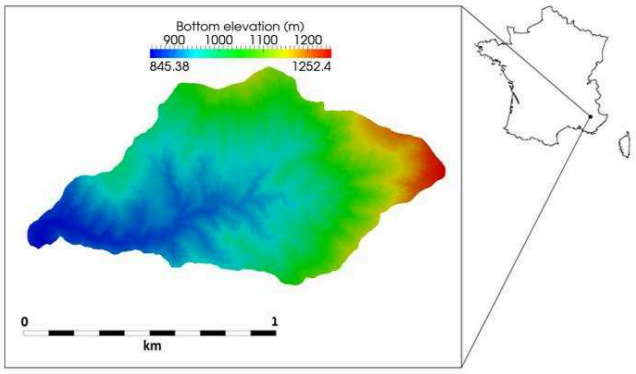

Figure 2 : Presentation of the Laval watershed

RESULTS

Plot scale erosion

For the first test case, the hydraulic results from TELEMAC-2D for a constant value of friction coefficient are presented on the Fig. 3. On this figure, the water depth and the Froude number are plotted. These results show a roll-wave phenomenon in the steep slope part of the domain. This phenomenon appears only under specific conditions of runoff flow. This is due to the soil disturbance when the Froude number is higher than 2. The waves reach a height of 2 mm when they are close to the break in slope and the water depth varies from 1 mm to 3 mm downstream. It is interessting to notice that the same roll-waves are observed with the variable friction model, but in this case, the wave period is higher.

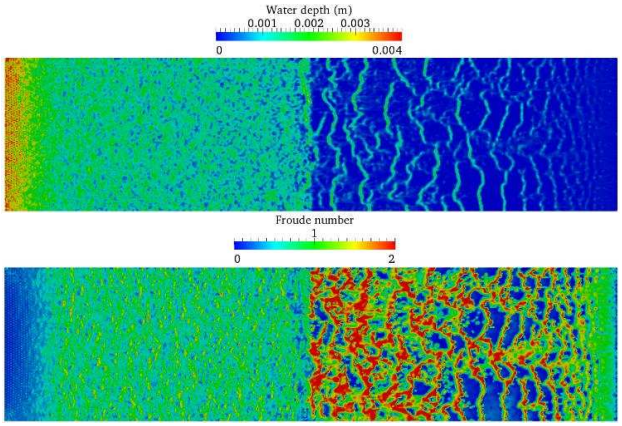

Figure 3 : Water depth and Froude number at the end of the simulation. The downstream boundary is on the left.

The main difference between the constant friction model and the variable one consists in estimating the bed shear stress. The Fig. 4 shows the calculated values of bed shear stress in the case of constant or variable friction coefficient. We can see higher values if the friction coefficient is calculated on each point, particularly in the upstream part. The maximal value of the shear stress is 1.35 Pa with the variable model, while it is only 0.93 Pa if the friction coefficient is constant.

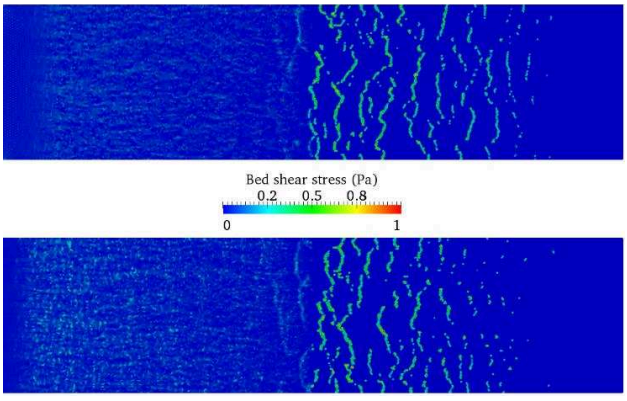

Figure 4 : Bed shear stress with the constant bottom friction model (at the top) and the variable one (at the bottom).

By coupling the model with SISYPHE, the bottom evolution is calculated and updated at each time step. The effects of the respective friction models on the bed evolution are compared on the Fig. 5. The models are compared first without adding specific terms for rain erosion. For both models, a rill erosion can be observed in the upstream part of the domain. In the case of a variable friction coefficient, the rills are deeper and visible even in the downstream part of the domain. This result is relevant regarding the previous conclusions on the bed shear stress values.

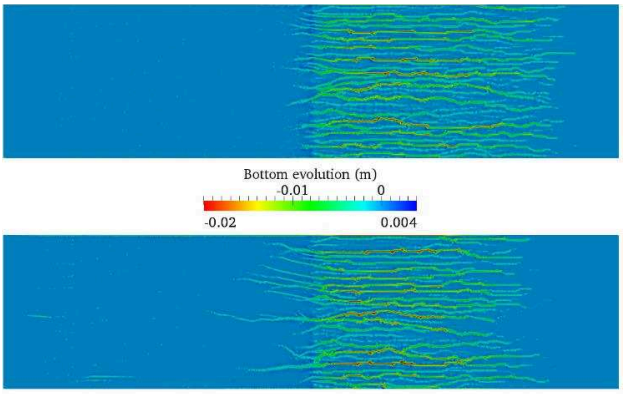

Figure 5: Bottom evolution without adding rain effect, using the constant friction model (at the top) or the variable one (at the bottom).

In order to test the four formulas defined in the part 1 for estimating the rain effect on the erosion term, a cross section is defined 20 cm upstream the break slope. On this cross section, the bed evolutions are compared after one hour of simulation for the four formulas (Fig. 6).

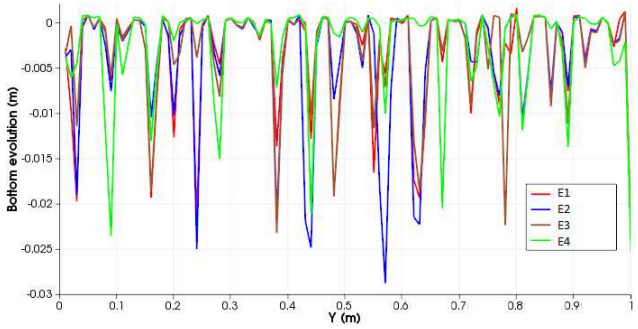

Figure 6 : Comparison of the bottom evolution between the rain detachment formulas on a cross section of the plot.

As a default set of parameters is available in FullSWOF_2D for the Hairsine and Rose model, the erodability parameters of each formula E1, E2 and E3 have been calibrated in order to obtain the same total volume with a constant friction value (at least the same order of magnitude). The Table 1 shows the computed volumes on the whole domain at the end of the simulation. Even if the computed volumes are comparable, the results of the Fig. 6 show that the rill formation is very different from one case to another.

An important point to notice is that the configurations SISYPHE+E4 and Hairsine & Rose evaluate the same rain effect with different source terms for flow erosion and deposition. In order to evaluate the impact of changing the flow detachment evaluation, these two configurations are compared on the same cross section (Fig. 7).

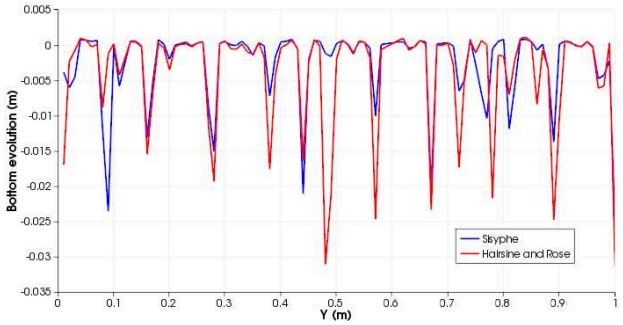

Figure 7 : Comparison between the SISYPHE+E4 and Hairsine and Rose models on a cross section of the plot

In this case, the rills are formed in the same place, even if their depth are frequently bigger with the Hairsine and Rose model. The effect of changing source terms for flow erosion and deposition is less significant than the one resulting of changing the rain effect at this scale.

The eroded and deposited volumes are presented in the Table 1 for all the tested combinations. We can notice that the use of a variable friction coefficient has no significant effect on the Hairsine & Rose model, but this effect is not negligible for the other configurations.

Especially, the configuration SISYPHE+E4 is very sensitive to the friction variations and this sensitivity not reliable with the other configurations. We can also notice that the rain detachment plays a significant role in the total erosion at this scale.

Model	Eroded volume	Deposited Volume	Total Volume
Constant friction			
SISYPHE	3.123	0.2545	-2.868
SISYPHE + E1	8.402	0.4717	-7.930
SISYPHE + E2	8.297	0.4725	-7.825
SISYPHE + E3	8.147	0.4719	-7.675
SISYPHE + E4	7.758	0.6283	-7.130
Hairsine and Rose	8.284	0.5234	-7.760
Variable friction			
SISYPHE	3.1490	0.3086	-2.840
SISYPHE + E1	10.51	0.3161	-10.19
SISYPHE + E2	10.38	0.3181	-10.07
SISYPHE + E3	10.34	0.3166	-10.02
SISYPHE + E4	5.064	0.1901	-4.874
Hairsine and Rose	8.105	0.4348	-7.671

Table 1 : Eroded and deposited volumes (10^{-3} m^3) computed at the end of the simulation for the first theoretical test case

River and adjoining hillslopes

In the second theoretical test case, the runoff causes roll-waves on the parcels when the Froude number is greater than 2, as it was observed in the first plot case. The Fig. 8 illustrates this result. Close to the river, the roll-waves reach about 1 cm height. In the channel, the flow is subcritical and it is slowed down by the flow conditions into the reservoir about 15 m before the entrance of the reservoir.

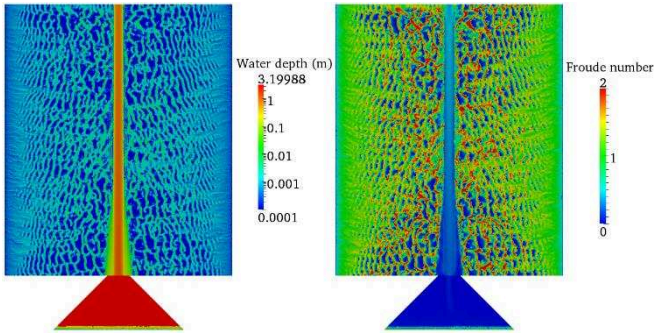

Figure 8 : Water depth and Froude number and the end of the simulation in the whole domain.

Depending on the chosen friction model (constant or variable), the Fig. 9 shows that the computation of the bed shear stress is this time again very different. Indeed, a homogenization is visible between the hillslopes and the river bed in the case of a variable friction coefficient. With a constant value of friction coefficient, the maximal value of the bed shear stress is 2 Pa on the hillslopes and 8 Pa in the river. If the friction coefficient depends on the water depth, it reaches a maximum value of 2 Pa in the river. We can also notice that the roll-waves period is higher with a variable coefficient, and that this phenomenon appears more upstream on the hillslopes.

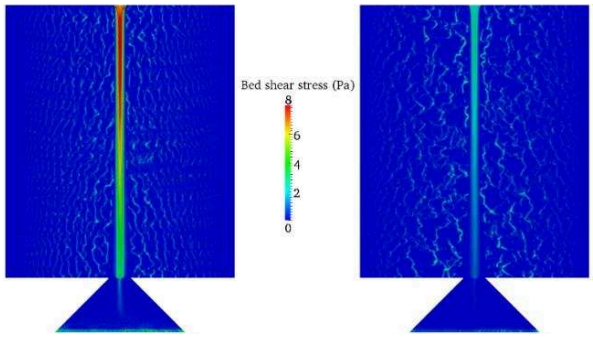

Figure 9 : Bed shear stress with the constant friction value (on the left) and the variable one (on the right)

The bottom evolution is first computed with the simple SISYPHE configuration (Fig. 10). We can observe that rills appear because of the runoff due to the rain on the hillslopes, and these rills are longer if the friction coefficient is variable. In terms of eroded volumes on the whole domain (Table 2), we can notice that the eroded volume is significantly higher with a variable friction coefficient. Concerning the deposition, whatever the characterisation of the friction coefficient is, it is located on the banks of the river, especially where the flow velocity starts slowing down.

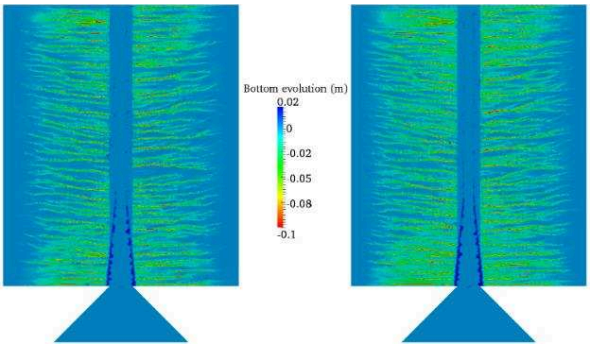

Figure 10 : Bottom evolution with the SISYPHE configuration, using the constant friction model (at the top) and the variable one (at the bottom).

As for the first test case, the four formulas Ei defined in the first part of this paper have been tested, using the same parameters than for the previous test case. The observed differences between SISYPHE+E1, E2 or E3 are very small (Table 2) and not significant with the simple SISYPHE configuration. This result can be explained by the dimensions of the eroded rills, which are much longer and deeper in this test case, and by the way more exposed to the flow erosion.

Because the main difference between the SISYPHE configurations and the Hairsine and Rose model consists in the erosion and deposition processes due to the flow, we can observe significant differences between these configurations in terms of global calculated volume (Table 2).

The Fig. 11 shows the bed evolution for the configurations SISYPHE+E4 and the Hairsine and Rose model, with a variable friction coefficient. The deposition appears to be more realistic with the Hairsine and Rose model, because it is very well correlated to the decrease of transport capacity. By using the Hairsine and Rose model, we can clearly observe a sediment transfer from the hillslopes to the reservoir. However, as it can be seen in the Table 2, the eroded volume is about two times bigger with the Hairsine and Rose model.

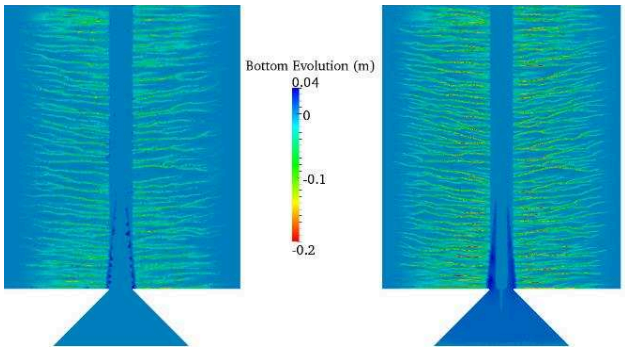

Figure 11 : Bottom elevation with the SISYPHE code (on the left) and with the Hairsine and Rose model (on the right)

For this test case, a last configuration has been tested. All the previous presented results are available by considering the main river bed as a non-erodible zone. The Fig. 12 presents the bed evolution obtained with the Hairsine and Rose configuration with an erodible river bed, by using a constant or a variable friction coefficient. These results show that the river bed erosion is higher when the friction coefficient is constant than when it is variable, as expected with the bed shear stress results in the Fig. 9. With the constant friction, the erosion in the river is about 1 m at the end of the simulation, while it is only 0.3 m with the variable friction model.

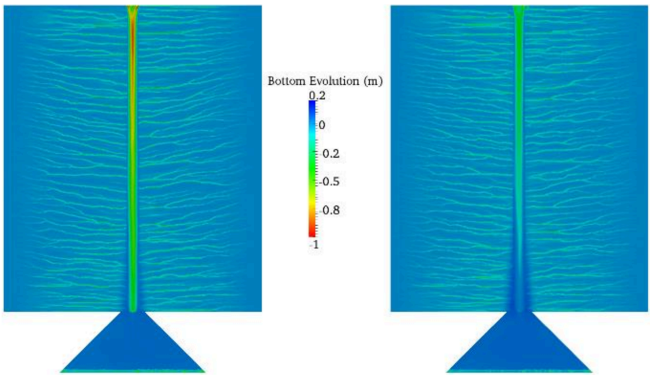

Figure 12 : Bed evolution obtained with the Hairsine and Rose configuration and an erodible river bed, with a constant friction on the left, and a variable one on the right.

The Table 2 summarizes the eroded volumes in the domain for the different tested configurations. The highest difference is visible between the Hairsine and Rose model and all the SISYPHE configuration. By using a variable friction coefficient, this difference tends to be decreased.

Model	Eroded volume	Deposited Volume	Total Volume
Constant friction			
SISYPHE	16.00	0.2969	-15.70
SISYPHE + E1	17.65	0.3794	-17.27
SISYPHE + E2	17.60	0.3812	-17.21
SISYPHE + E3	17.55	0.3769	-17.17
SISYPHE + E4	16.16	0.3078	-15.86
Hairsine and Rose	30.78	1.677	-29.11
River erosion	57.25	7.132	-50.12
Variable friction			
SISYPHE	20.58	0.3289	-20.25
SISYPHE + E1	21.82	0.4806	-21.34
SISYPHE + E2	21.89	0.4694	-21.42
SISYPHE + E3	22.02	0.4891	-21.53
SISYPHE + E4	20.72	0.3324	-20.38
Hairsine and Rose	28.63	3.438	-25.19
River erosion	50.03	9.126	-40.91

Table 2: Eroded and deposited volumes (m^3) calculated on the whole domain for the second theoretical test case

The Laval catchment

First a constant one-hour rain is applied on the whole watershed in order to evaluate the new developments by the same way than the two previous test cases. The Fig. 13 shows the results in terms of water discharge and suspended sediment concentration at the outlet of the catchment, for the constant and the variable friction coefficient model.

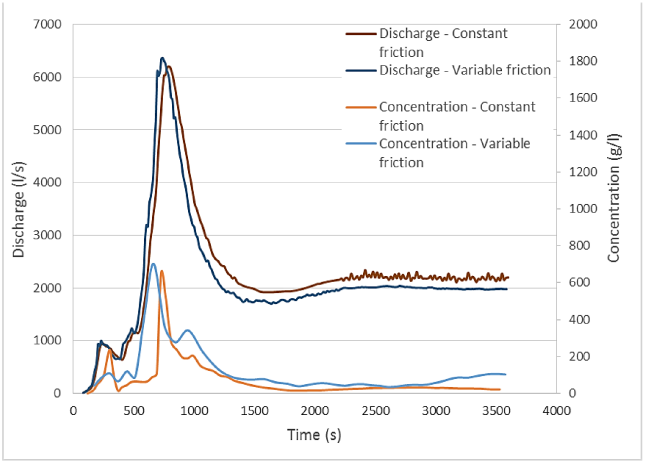

Figure 13 : Discharge and concentration at the outlet depending on the friction model

We can see on this figure that the variation of the friction coefficient does not have a significant effect on the discharge at the outlet. When the flow is stabilized, the flow rate is lower for the variable friction coefficient and presents no high-frequency variations.

On the opposite, the choice of the friction model has a significant impact on the suspended sediment concentration signal. The results on the Fig. 13 show that even if the magnitude of the maximum value is the same for both models, the shapes of the two signals are very different: with a variable friction coefficient, the arrival time of the maximum value is smaller, and the signal presents a second significant peak value.

The Fig. 14 shows the bed shear stress in the watershed at the end of the simulation, when the flow is stabilized. Unlike the results for the two theoretical test cases presented previously, a preferential flow is already created in the watershed.

Thus, the velocities are increasing along the river and its tributaries, as well as the bed shear stress values. In analogy to the second theoretical test case, the shear stress is smaller in the river bed with a variable friction coefficient than with a constant one.

Indeed, the value of the bed shear stress with the constant friction coefficient can exceed 100 Pa at some points and is globally around 50 Pa in the main river. With the variable friction model, the mean value of the bed shear stress in the main river is about 15 Pa and it can reach at most 30 Pa.

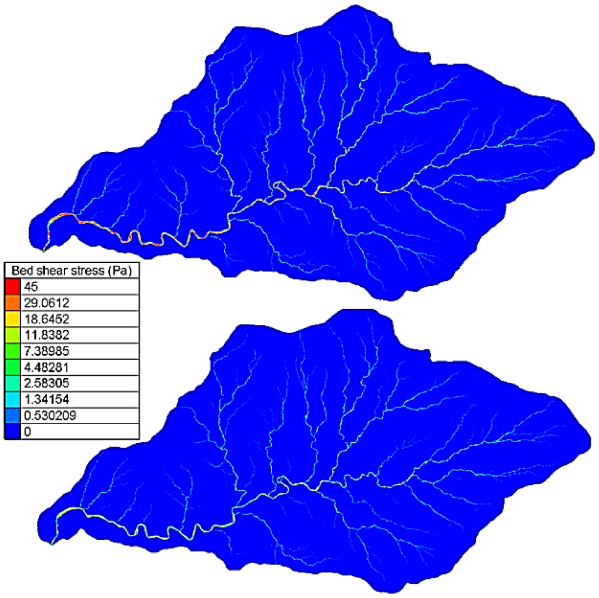

Figure 14 : Bed shear stress distribution in the watershed with constant friction coefficient (at the top) and with variable friction coefficient (at the bottom)

The bottom evolution, plotted on the Fig. 15, follows the bed shear stress results obtained in the domain. The main part of the erosion is located in the river network and the constant friction model gives the deepest erosion values.

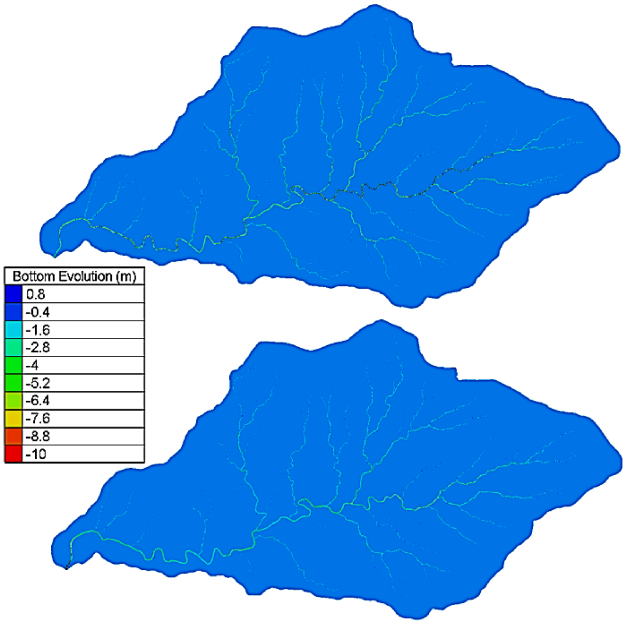

Figure 15 : Bottom evolution in the watershed with constant friction coefficient (at the top) and with variable friction coefficient (at the bottom)

The erosion is superior to 10 m in the main river for the first model and it is at most 4 m for the second. On the other hand, the erosion is quite similar in the tributaries with the two friction models, starting to be significant at the same points upstream and with a comparable depth.

The Fig. 16 shows the concentration at the outlet for the SISYPHE model, the SISYPHE model with the E4 formula and the Hairsine and Rose model. These simulations are performed with the variable friction coefficient model. The concentration are higher with the Hairsine and Rose model. The effect of the rain detachment formula is in this case negligible when the SISYPHE model is used.

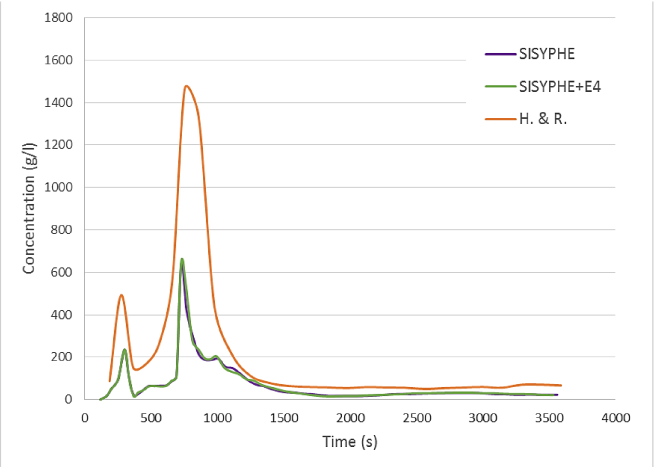

Figure 16 : Suspended sediment concentration at the outlet of the Laval watershed for the constant rain

The Table 3 gives the total eroded volume in the domain in function of the choice of the friction coefficient calculation (constant or variable), the rain detachment formula and the flow erosion/deposition model.

Model	Eroded volume	Deposited Volume	Total Volume
Constant friction			
SISYPHE	45214	280	-44934
SISYPHE + E1	45490	282	-44207
SISYPHE + E2	45514	283	-45230
SISYPHE + E3	45517	286	-45232
SISYPHE + E4	45530	282	-45248
Hairsine and Rose	35036	206	-34831
Variable friction			
SISYPHE	25278	366	-24912
SISYPHE + E1	28387	386	-28001
SISYPHE + E2	28495	381	-28113
SISYPHE + E3	28083	375	-27708
SISYPHE + E4	28628	382	-28246
Hairsine and Rose	28630	344	-28286

Table 3: Eroded and deposited volumes (m^3) calculated on the whole domain for the Laval watershed

The effect of the erosion terms due to the rain is negligible with the SISYPHE model when the friction coefficient is

constant. The models SISYPHE+Ei are more sensitive to the different formulas with a variable friction coefficient. But whatever the friction model is, the choice of the rain formula has not a significant impact on the results in terms of total eroded volume. In the two theoretical test cases, the erosion volumes increased with the variable friction model while it is the contrary at this scale.

The model has also been tested on two real hydrological events, and the water discharges and sediment concentrations have been compared at the outlet of the watershed with the field measurements. The calibration is realized with one event and the same parameters are used for the second one. For the hydraulic model, the variable friction model is used and the height of the soil roughness k is modified in function of the areas (river bed or hillslope).

The Fig. 17 shows as a function of time the hydraulic results of the model for the two rainfall events, compared with the measured hydrograph and presented with the associated rain signal.

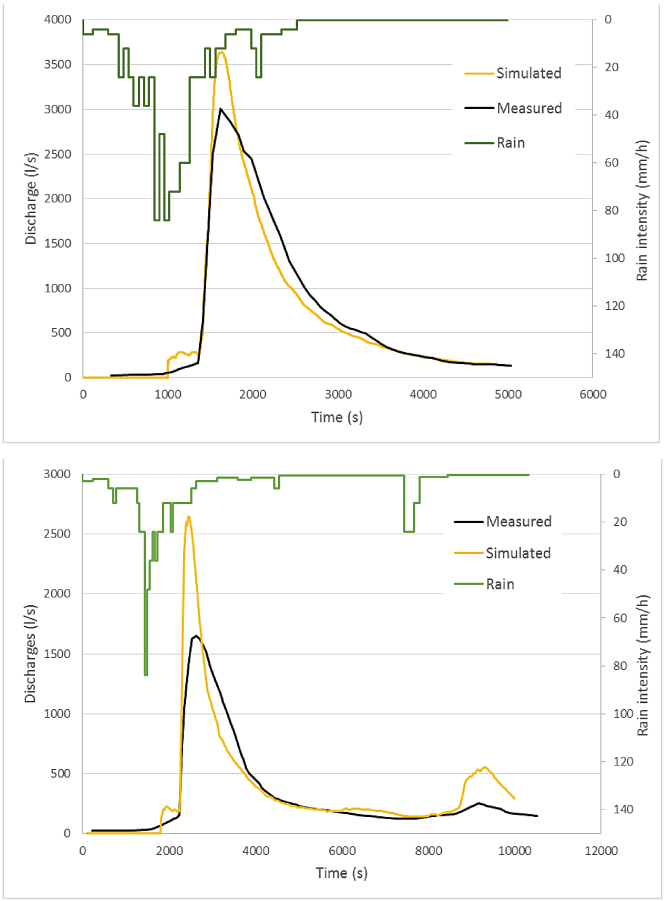

Figure 17 : Discharge at the outlet of the Laval watershed for the two rain event

We can see on this figure that the discharge peak is reproduced at the same time, but the maximum value is much higher than the measured ones for the two events. With SISYPHE, the calibration of the model has been done with the lateral and longitudinal dispersion coefficient of the convection-diffusion equation and the grain size. The respective calibrated values for these parameters are $K_x = 10\ m^2/s$, $K_y = 10\ m^2/s$ and $D_{50} = 70\ \mu m$.

Once this calibration completed, the four rain detachment formulas are tested with the same erodability coefficient as the previous test cases. In the Fig. 18, the outlet concentration are represented with the different models.

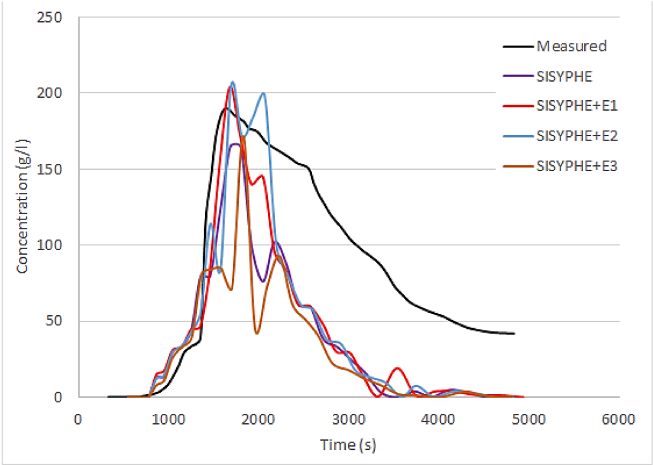

(a) SISYPHE + Ei, Event 1

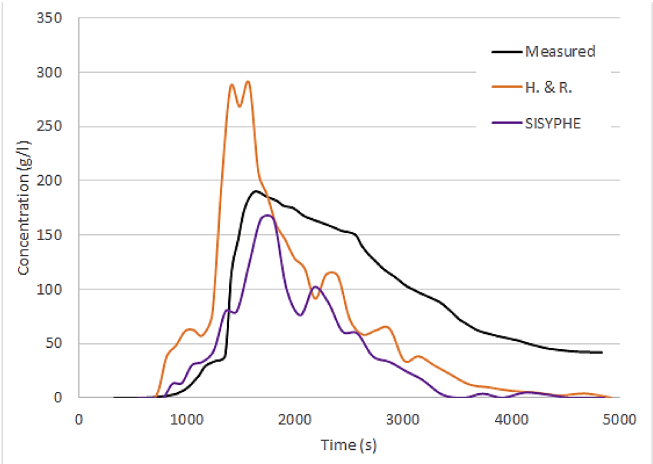

(b) SISYPHE+E4 and Hairsine and Rose, Event 1

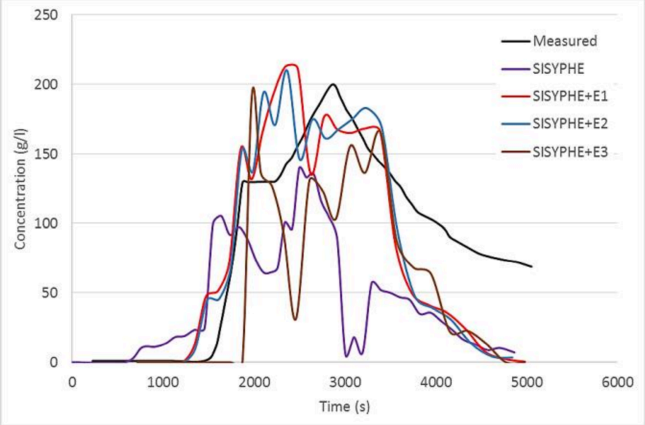

(c) SISYPHE + E1, Event 2

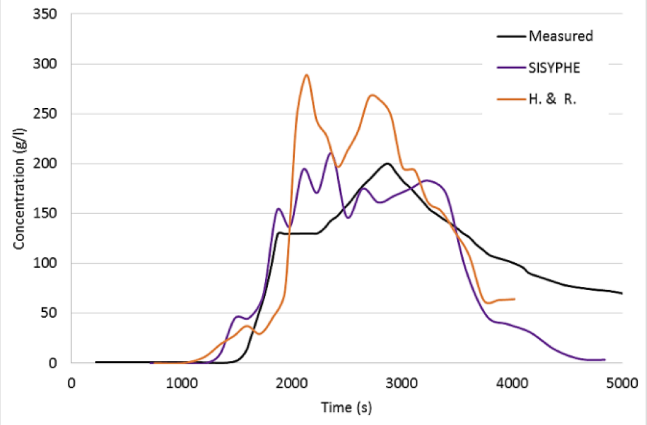

(d) SISYPHE+E4 and Hairsine and Rose, Event 2

Figure 18 : Sediment concentration at the outlet of the Laval watershed

The previous graphs show that:

- the choice of the rain-erosion formula is of a great importance for reproducing correctly the suspended sediment concentration signal. In this case, the formulas E1 and E4 appear to be the most relevant formulations. Without rain detachment formulas, SISYPHE is unable to reproduce correctly the concentration signals, especially for the second event;
- The parameters used for the formulas Ei at the plot scale allow reproducing the right order of magnitude for the suspended sediment concentration signal, with a calibrated value of sediment diameter which is low but still realistic;
- The erosion/deposition model for the flow part has a great impact on the concentration values. Both SISYPHE and Hairsine and Rose models are able to reproduce quite well the concentrations at the outlet, but the curves are decreasing too fast after the peak, whatever the parameter are modified. Furthermore, the Hairsine and Rose model overestimates the suspended concentration with this set of parameters, which is very complicated to change without losing the physical meaning of the whole set of parameters.

DISCUSSION

The great interest of the variable friction model is to reproduce continuously the flow and the erosion on a miscellaneous domain. Indeed, for an application on a real watershed, where the hillslope runoff, the river flow and the deceleration of the water in a reservoir are all observed, this approach allows a better representation of the different processes. Moreover, this friction characterization had been compared to a large number of existing models in [2], with similar results. Nevertheless, several studies ([9], [10]) show that for smaller range of inundation ratio (Λ), the model can be significantly improved. Furthermore, there are three equations to describe the Darcy-Weisbach coefficient depending on the inundation ratio, and the boundary between these equations can be different (see [11]). The highest difficulty is to give the best value of the size in the soil roughness, the k coefficient in the definition of the inundation ratio, especially in a large domain.

With the increasing scale, we observed in this work that the flow detachment becomes predominant over the rain detachment. The difference in the eroded volumes between the simulation of the SISYPHE flow detachment alone and SISYPHE with the rain erosion formulas becomes smaller (see Table 1 and Table 2). The fact that one class of non-cohesive sediments is used with a relatively small grain size (150 µm, and 70 µm for the calibrated value) can overestimate the erosion by the flow compared to the rain erosion. Another hypothesis is that the the rain drop impact adds mass in the deposited layer, which is easily detached by the flow, like it is presented in the Hairsine and Rose model. In this case, the SISYPHE erosion/deposition system does not represent this indirect effect of the rain detachment. Another simulation choice that could be responsible of this results is that the mesh size enlarge with the scale (1cm, 15 cm and 1 m). Indeed, the disturbance of ± 1 mm at each node of the mesh is distributed with a different gap and may have a different effects. With a very small mesh at the larger scale, the cumulative differences observed with the different rain formulas may give a higher importance to the choice of the rain detachment formula.

In addition, many phenomenon are not represented in the simulations. As the matter of fact, the infiltration, exfiltration and evapotranspiration are not taken into account. It could explain the excess of maximum discharge in the calibration of the hydraulic model of the Laval catchment (Fig. 16). In order to have better results and for other rainfall events, it could be essential to represent these processes, that are usually not defined at the mesh scale. Furthermore, the influence of the vegetation on both erosion and runoff is not represented, despite its predominant impact (see [12]). The effect of

vegetation may better improve the diffusion or retention effect observed on suspended sediment concentration. Some other phenomenon like debris flow or landslide which could transport substantial amount of sediment are also not described. These kind of rare events are difficult to predict, so their modeling is very complicated.

CONCLUSION

The V7P0 version of TELEMAC-SISYPHE contains mostly equations adapted to the river or coastal erosion. Inspired by existing codes used for modeling plot erosion, some implementations have been realized in this code in order to simulate the sediment transport in an entire watershed and create a continuity between the hillslopes and the river bed. Three test cases have been chosen or defined for analyzing the effect of these new developments at different scales.

A variable friction model, depending on the water depth at each point of the mesh, has been tested. The main interest of this model is the homogenization created between the hillslope and the river erosion, with a low impact on the total eroded volumes. Its main effect is to moderate the river erosion which becomes more realistic, and to allow a better transfer from the plots to the outlet.

Four rain detachment formulas have also been added to the SISYPHE flow detachment. At the local scale, where the power of the flow is low, the effect of the rain detachment is considerable, so the choice of the rain formula significantly impacts the erosion results. However, at a largest scale, the choice of the rain detachment formula is less influent in term of erosion volumes, but is still very important in terms of shapes of the suspended sediment concentration signal.

At the same time, an erosion model designed for plot, the Hairsine and Rose model, has been carried out to be compared with the erosion/deposition terms of SISYPHE. The erosion results are very different, especially in the cases with a flow strong enough to be preponderant. For example, the H&R model overestimates the suspended concentration at the outlet of the Laval watershed. The parameter set, which is very large, is complicated to calibrate, especially for a complex and heterogeneous real case.

A large variety of options to model erosion at the watershed scale has been given in this paper, but there are still further ways to explore. The question of chosing the best numerical schemes, for both hydraulic and sediment transport, is still open. The infiltration and evapotranspiration processes, as well as the influence of the vegetation on runoff and erosion should also be represented. Finally, representing only one class of suspension transport may not be enough to describe all the processes existing on a real watershed, and the evaluation of the bed load transport appears to be also an important issue. With a better description of these still-missing processes, the code will be able to be used in the future for preventing the erosion on a watershed and finding up-front solution, like hillslopes management in area with dam protection issues.

REFERENCES

[1] P. Tassi, C. Villaret, “Sisyphe V6P3 User’s Manual”, Note EDF LNHE ref. H-P74-2012-02004-EN, January 2014.

[2] D. S. L. Lawrence, “Macroscale surface roughness and frictional resistance in overland flow”, Earth Surface Processes and Landforms, Vol 22, Issue 4, pp. 365–382, April 1997.

[3] G. Nord, M. Esteves, “PSEM_2D: A physically based model of erosion processes at the plot scale” Water Resources Research, Vol. 24, Issue 13, pp. 1766–1780, June 2010

[4] C. A. G. Santos, V. S. Srinivasan, K. Suzuki, M. Watanabe, “Application of an optimization technique to a physically based erosion model” Hydrological Processes, Vol. 17, Issue 5, pp. 989–1003, April 2003.

[5] R. P. C. Morgan, J. N. Quinton, R. E. Smith, G. Govers, J. W. A. Poesen, K. Auerswald, G. Chisci, D. Torri, M. E. Styczen, “The European Soil Erosion Model (EUROSEM): a dynamic approach for predicting sediment transport from fields and small catchments”, Earth Surface Processes and Landforms, Vol. 23, Issue 6, pp. 527–544, June 1998.

[6] M. H. Le, “Modélisation multi-échelle et simulation numérique de l’érosion des sols de la parcelle au bassin versant”, Université d’Orléans, <tel-00838947>, November 2012, French.

[7] P. B. Hairsine, C.W. Rose, “Rainfall Detachment and Deposition: Sediment Transport in the Absence of Flow-Driven Processes”, Soil Science Society of America Journal, Vol. 55 No. 2, pp. 320-324, March 1991.

[8] C. Le Bouteiller, S. Klotz, F. Liébault, M. Estèves, Observatoire hydrosédimentaire de montagne Draix-Bléone, Irstea, 2015, http://dx.doi.org/10.17180/OBS.DRAIX.

[9] D. S. L. Lawrence, “Hydraulic resistance in overland flow during partial and marginal surface inundation: Experimental observations and modeling”, Water Resources Research, Vol. 36, Issue 8, pp. 2381–2393, August 2000.

[10] V. Ferro, “Flow resistance in gravel-bed channels with large-scale roughness”, Earth Surface Processes and Landforms, Vol. 28, Issue 12, pp. 1325-1339, November 2003.

[11] N. Roche, “Modélisation du ruissellement sur surfaces rugueuses” Hydrology. Université Joseph-Fourier - Grenoble I, <tel-00121568>, December 2006.

[12] N. Claude, “Interactions entre végétation, processus hydro-sédimentaires et morphodynamique des cours d'eau : état de l'art et principes de modélisation”, Note EDF LNHE ref. H-P73-2014-05213-FR, January 2015.